Comparative Study on Chemical Kinetics Mechanisms for Methane-Based Fuel Mixtures under Engine-Relevant Conditions

Amin Paykani

School of Physics, Engineering and Computer Science, University of Hertfordshire, Hatfield AL10 9AB, UK;
a.paykani@herts.ac.uk

Abstract: The use of natural gas in pure or in a blended form with hydrogen and syngas in spark ignition (SI) engines has received much attention in recent years. They have higher diffusion coefficient and laminar flame speed, a small quenching distance and wider flammability limit which compensate the demerits of the lean-burn natural gas combustion. Therefore, a careful examination of the chemical kinetics of combustion of gaseous fuel blends is of great importance. In this paper, performance of the various chemical kinetics mechanisms is compared against experimental data, accumulated for methane-based fuel blends under engine-relevant conditions to find the most appropriate mechanism in engine simulations. Pure methane, methane/syngas, and methane/propane blends are mainly studied at various temperatures, pressures, and equivalence ratios. The ignition delay time and laminar flame speed are used as quantitative metrics to compare the simulation results with the data from experiments. The mechanisms were shown to be mainly consistent with the experimental data of lean and stoichiometric mixtures at high pressures. It was also shown that the GRI-3.0 and 290Rxn mechanisms have high compatibility with the ignition delay times and laminar flame speed at high pressures and lean conditions, and they can be utilized for simulations of SI engine combustion due to their lower computational cost. The results of present research provide an important contribution to the methane-based fuel blends combustion simulation under SI engine-relevant conditions.

Keywords: ignition delay time; laminar flame speed; natural gas; engine-relevant condition; mechanisms

1. Introduction

Internal combustion (IC) engines are commonly used as the main propulsion system for air, ground, and rail vehicles. The use of fossil fuels for these engines often raises concerns about the environment and pollutants from combustion. Therefore, the use of alternative fuels, such as natural gas, has received much attention in recent years due to their unique properties in improving the performance and reducing emissions of IC engines [1–3]. Additionally, the high octane number and high knock resistance of natural gas allows to run the SI engine on higher compression ratios [4]. Moreover, lean natural gas combustion has shown the potential to improve efficiency compared to stoichiometric gasoline engines, but suffers from unstable and poor ignitability of the fuel–air mixture, leading to incomplete combustion or misfire [5]. The reduction of flame speed at lean operation results in significant cycle-to-cycle variations (CCV) [6–8].

Hydrogen and syngas are considered a suitable candidate as additive for lean-burn natural gas fueled SI engines, due to its higher laminar flame speed, wider flammability limits and small quenching distance [9–11]. Syngas derived from natural gas, coal, biomass, or hydrocarbon feedstock, is primarily consisted of hydrogen and carbon monoxide, which has also been considered as a future fuel for IC engines, since in addition to offering similar advantages as hydrogen it can also be produced on-board through fuel reforming [12,13]. There is another interesting alternative transportation fuel which is Propane (C_3H_8), and it

is also identified as liquefied petroleum gas (LPG) with high-energy density and relatively low cost [14]. Propane is the smallest alkane with cool flame and negative temperature coefficient (NTC) under engine-relevant conditions [15,16]. The physicochemical properties of the studied gaseous species are provided in Table 1.

Table 1. Physiochemical properties of the studied gaseous species [17,18].

Properties	Unit	CH$_4$	C$_3$H$_8$	H$_2$	CO
Molecular weight	(g/mol)	16.04	44.1	15.0	28.01
Density at 0 °C and 1 atm	(kg/m^3)	0.72	1.88	0.09	1.25
Specific gravity at 0 °C and 1 atm	-	0.55	1.52	0.06	0.96
Stoichiometric air–fuel ratio	mass basis	17.2	15.5	34.1	0.57
Wobbe number	(MJ/Nm^3)	45	67.8	44.2	12.4
Flammability limit, % volume of fuel in air	volume of air	5–15	2.1–9.5	4–75	12–75
Laminar flame speed at 1 atm and 300 K, Φ = 1	(cm/s)	30	38	180	35
Adiabatic flame temperature	(°C)	1963	1980	2210	2121
Auto-ignition temperature	(°C)	585	455	560	610

Many researchers have studied the auto-ignition of methane and its blends at different operating conditions [19–22]. Hu et al. [23] assessed experimentally and computationally laminar flame speeds and ignition delay times of methane–air mixtures. The GRI-Mech 3.0, USC Mech II, and Aramco Mech 1.3 mechanisms were validated at higher pressures (up to 10 atm). For estimating ignition delay times of fuel at lean and stoichiometric mixtures at high pressure the Aramco Mech 1.3 gave good predictions. Lee at al. [24] used Cantera to conduct a comprehensive comparison of Davis2005, GRI1999, USC2007, NUIG2013, Sun2007, and Li2007 chemical kinetics mechanisms and published experimental results for mixture compositions that are pertinent to biogas/syngas mixtures. They discovered that the NUIG2013 mechanism is the best fit for reproducing the calculated laminar flame speed and ignition delay time of biogas/syngas fuel blends. It can replicate the experimental results for the majority of mixture compositions. Fischer and Jiang [25] assessed five comprehensive reaction mechanisms for simulation of ignition delay times of CH$_4$-CO-H$_2$-CO$_2$ fuel mixtures by employing Homrea software. The NUIG mechanism showed to be the best choice for simulating the burning of bio-syngas.

There is no detailed analysis of various pathways for assessing ignition delay times and laminar flame speeds of methane-based fuels under lean-burn natural gas SI engine conditions, according to the literature (i.e., for initial pressures between 10 and 40 bar, temperatures between 900 and 1600 K, and air–fuel equivalence ratios from 0.5 to 0.8). In our study, ignition properties of methane, methane/syngas, and methane/propane mixtures are compared at high-pressure engine-relevant conditions using most relevant and state-of-the-art chemical mechanisms. Finally, the best mechanism that could serve as suitable candidate for future natural gas SI engine simulations is suggested.

2. Kinetic Modeling Approach

Simulations were carried out using the Cantera reactive flow open source code [26] for the seven mechanisms specified in Table 2. These mechanisms are the most accepted kinetic models for simulating methane ignition delay times and laminar flame speed in the literature. NUIG3 is a large-scale, hierarchical-structured system that accounts for the combustion of C1–C5 hydrocarbons. It is the result of a long-term project to develop a model capable of describing the combustion of different hydrocarbons under a variety of conditions. The AramcoMech 1.3 mechanism describes hydrogen combustion and its mixtures with carbon monoxide (syngas), followed by C1–C2 hydrocarbon combustion. This model was validated using flow reactors, shock tubes, jet-stirred reactors, and flame tests, over a wide range of initial conditions. The USC Mech II integrates recent thermodynamic, kinetic, and species transport updates related to high-temperature oxidation of hydrogen, carbon monoxide, and C1–C4 hydrocarbons. Note that this mechanism was not tested

for methane ignition delay times; also it was tested only for low pressure conditions. The 290Rxn mechanism was successfully used to predict the ignition properties of biogas and syngas fuel mixtures, as well as natural gas with impurities such as ethane and propane. Wang's skeletal mechanism is much suitable for high-temperature combustion of H_2, and C1−C4 hydrocarbons. The San Diego (UCSD) Mechanism has been validated for combustion of hydrogen, carbon monoxide, methane, ethane, acetylene, propane, methanol, and ethanol with experimental data. Based on flame speed measurements and shock tube experiments, the GRI-Mech 3.0 was optimized and tested for methane and natural gas over a broad range of conditions, including a temperature range of 1000–2500 K and a pressure range of 10 Torr to 10 atm. While its performance for high pressure and lean condition operation in combustion engines for different blends of natural gas has not been studied. Wang's skeletal mechanism was developed from a detailed mechanism for high-temperature combustion of H_2, and C1–C4 hydrocarbons.

Table 2. The used chemical kinetic mechanisms.

Mechanism Name	Number of Species	Number of Reactions	Reference
NUIG3	293	2928	[27,28]
AramcoMech1.3	253	1542	[29]
USC Mech II	111	784	[30]
290Rxn	72	290	[31]
San Diego	70	321	[32]
Wang	56	428	[33]
GRI-Mech 3.0	53	325	[34]

3. Results and Discussion

From the literature, a complete collection of experimental results was extracted to validate calculations by Cantera and compare the simulation results. Ignition delay times and laminar flame speeds were computed using a 0D perfectly stirred reactor (PSR) model and 1D laminar premixed flames, respectively. Table 3 summarizes the experimental data for ignition delay time and laminar flame speed of methane, methane/syngas and methane/propane mixtures under engine-like operating conditions obtained from previous studies.

3.1. Methane

The predicted ignition delay time for CH_4 as a function of temperature is indicated in Figures 1 and 2 for different pressures and equivalence ratios. Results are compared with the previous published works and a good agreement with experimental results is gained. Temperature effect on ignition delay time is very important as described by the Arrhenius correlation (i.e., $\tau = A.p^a \phi^b X_{O_2}^c \exp \frac{E_a}{RT}$). With a rise in temperature, ignition delay times decrease in all conditions. With increasing pressure, the concentration of reactants (i.e., reactivity) increases, resulting in a shorter ignition delay period. In general, for a standard hydrocarbon fuel, the pressure exponential (*a*) gives a negative value, implying that ignition delays decrease as pressure increases. Pressure, on the other hand, has an effect on methane oxidation; as pressure increases, the concentration of reactants (CH_4 and O_2) rises, resulting in a decrease in auto-ignition delay times, as shown by the sensitivity analysis in previous studies [35,36]. It is also seen that the impact of pressure on ignition delay becomes prominent especially at high temperature conditions due to acceleration of chain branching reactions at high temperatures.

Based on the results of Petersen et al. [37], Aramco 1.3 and NUIG3 mechanisms have good prediction in ignition delay at *p* = 20 atm and *T* > 1380 K, but at low temperatures, GRI 3.0 and USC II provide much accurate predictions. Moreover, GRI 3.0 and UCSD mechanism behave well for low temperature ignition at *p* = 50 atm. According to the experimental results of El Merhubi et al. [38], for both equivalence rations, GRI 3.0 and UCSD mechanisms have good prediction in ignition delay at *p* = 40 bar and *T* < 1530 K.

The discrepancy between simulations and experiments is due to the uncertain elementary reaction rate constant and different used facilities. Figure 3 depicts the relative error of simulation from experiments for methane ignition delay time at p = 40 bar, ϕ = 0.5. The agreement between experimental and simulation results was calculated using the following equation:

$$\overline{E_i} = \frac{1}{N_i} \sum_{j=1}^{N_j} \left| \frac{Y_{sim,ij} - Y_{\exp,ij}}{Y_{\exp,ij}} \right| \times 100\% \tag{1}$$

As can be seen, a recommended prediction values for ignition delay time is obtained using GRI-Mech 3.0 at lean, lower temperatures and high pressures. AramcoMech 1.3 and NUIG3 mechanisms over-predict ignition delay time especially at stoichiometric conditions.

Table 3. Experimental conditions for the ignition delay time and laminar flame speed simulation of CH_4, $CH_4/H_2/CO$, and CH_4/C_3H_8 mixtures at high pressures reported in the literature.

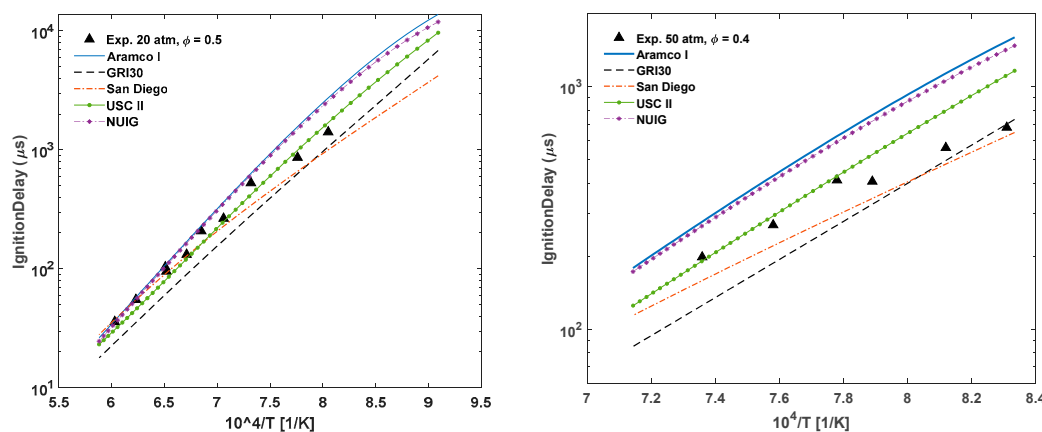| Mixture	ϕ	p (atm)	T (K)	Reference
	Ignition delay time			
100%CH_4	0.5	~20	1250–1650	[39]
100%CH_4	0.5/1.0	~10 to 40	1400–2000	[38]
100%CH_4	0.4	~50	1200–1350	[37]
50%$CH_4$30%$H_2$20%CO	0.5	~50	950–1100	[40]
90%$CH_4$10%C_3H_8	0.5	~10 to 30	1200–1500	[41]
	Laminar flame speed			
100%CH_4	0.6–1.4	~2 to 60	298	[42]
40%CH_4 30%$H_2$30%CO	0.8–1.6	~1	295	[43]

Figure 1. Comparison of methane ignition delay time for different mechanisms with the experimental data: **left**: p = 20 atm and ϕ = 0.5 [44]; **right**: p = 50 atm and ϕ = 0.4 [37].
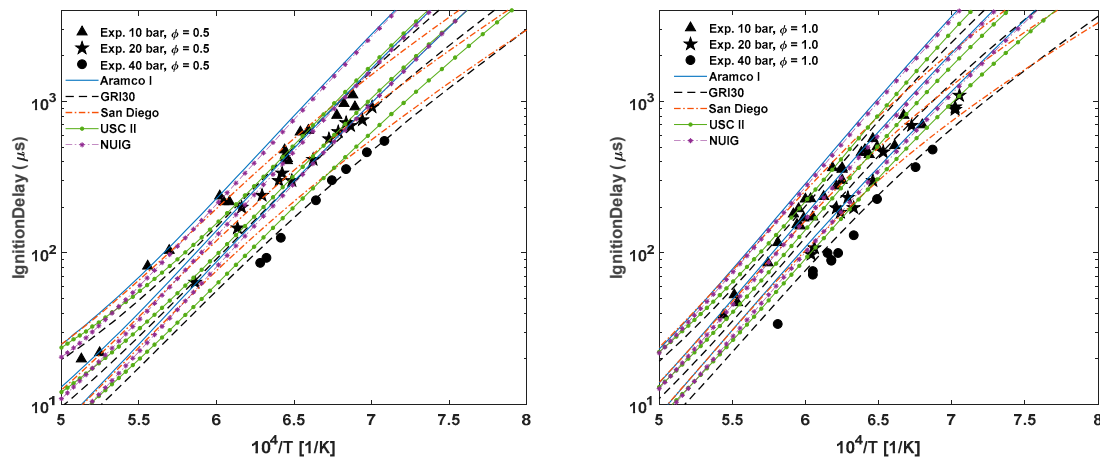
Figure 2. Comparison of methane ignition delay time for different mechanisms with the experimental data at *p* = 10, 20, 40 bar and, **left**: ϕ = 0.5; **right**: ϕ = 1.0 [38].
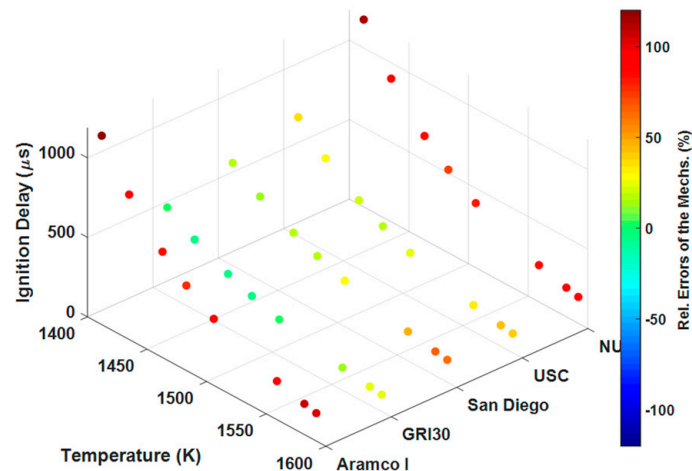

Figure 3. The relative error of simulation from experiments for methane ignition delay time (*p* = 40 bar, ϕ = 0.5).

The simulation findings corresponding to the calculated laminar flame speed of CH$_4$ [42] at different pressures ranging from 2 to 60 atm has been indicated in Figure 4. All of the mechanisms were found to be able to capture the impact of pressure on the laminar flame speed at higher pressures. Firstly, it is evident that by increasing pressure laminar flame speed decreases. Secondly, for *p* < 20 atm, there is an inconsistency between numerical and experimental results at lean and rich operating conditions. For lower pressures Aramco 1.3 and NUIG mechanisms perform well in prediction of laminar flame speed. For pressures higher than *p* = 40 atm, the deviation between numerical and experimental results is much considerable. However, AramcoMech1.3 mechanism shows an acceptable prediction behavior compared to other mechanisms. A slightly higher flame speed compared to the other mechanisms for rich mixtures has been expected by the NUIG3 mechanism. By computing the relative error for each mechanism for *p* = 40 atm, the GRI 3.0 mechanism was found to yield the best performance for lean and stoichiometric condition (see Figure 5), while Aramco 1.3 and UCSD mechanisms provide more accurate results at rich conditions. NUIG and GRI 3.0 over-predict laminar flame speed at rich conditions. The large deviation of USC II mechanism is due to the fact that it was tuned for high temperature applications.
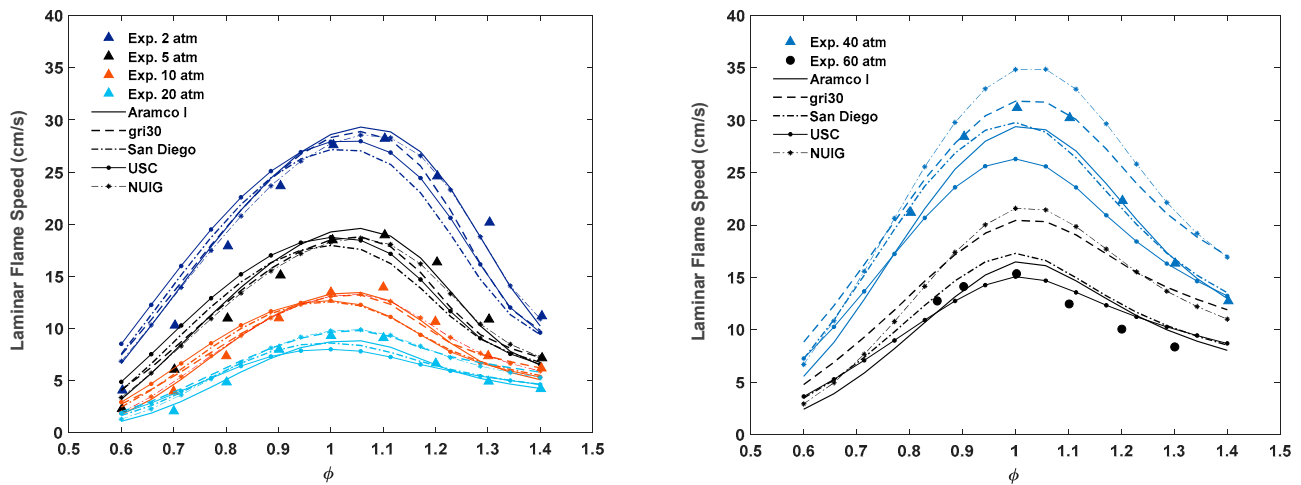
Figure 4. Comparison of laminar flame speed with the experimental data; **left**: CH_4/air mixtures p = 2, 5, 10, 20, **right**: CH_4/O_2/He mixtures p = 40 and 60 atm as a function of equivalence ratio, T_{ini} = 298 K [42].
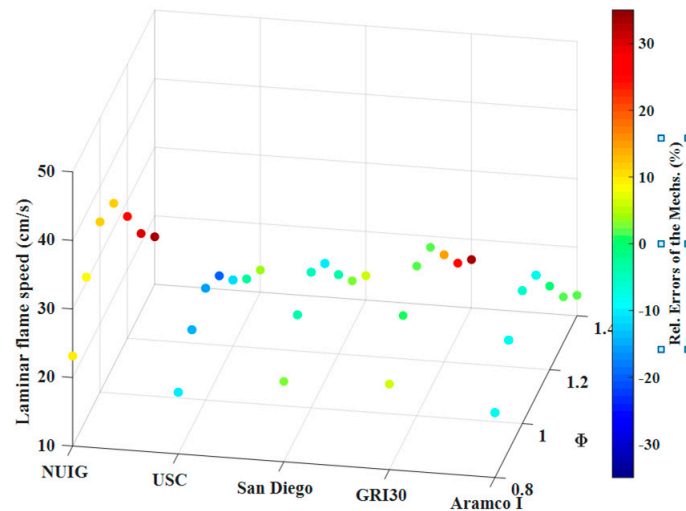

Figure 5. The relative error of simulation from experiments for CH_4/O_2/He mixtures laminar flame speed (p = 40 bar, T = 298 K).

3.2. Methane/Syngas Mixtures

Comparison of ignition delay time for 50%CH_4/30%H_2/20%CO mixtures high pressure and lean conditions for different mechanisms is demonstrated in Figure 6a. It can be seen that there is a good agreement between the simulation and experiments results especially at lower temperatures. The results obtained suggest only a trivial effect of CO addition on ignition delay of CH_4/H_2 mixtures which is in consistent with the results of Gersen et al. [40]. Figure 6b shows the relative error of simulation from experiments for methane/syngas mixture ignition delay time at p = 50 bar, ϕ = 0.5. It is obvious that GRI 3.0, UCSD and USC II mechanisms provided much accurate predictions of ignition delay time for methane/syngas blend at high pressure and low temperatures.

Comparison of laminar flame speed for different CH_4/H_2/CO mixtures at 1 atm pressure for different mechanisms is demonstrated in Figure 7. Since there is no relevant laminar flame speed data at elevated engine-like pressures in the literature, we conducted the simulations at 1 atm pressure. It is evident that all mechanism under-predict laminar flame speed value at rich condition, but there is a good agreement between simulations and experiments at lean condition. In addition, the location of maximum flame speed shifted towards richer mixtures when syngas fraction was increased, which is due to the greater

influence of the increasing flame temperature on flame speed. By computing the relative error for each mechanism, the GRI 3.0 and UCSD mechanisms were found to yield the best predictions for lean condition, while NUIG3 gives better results at rich condition.
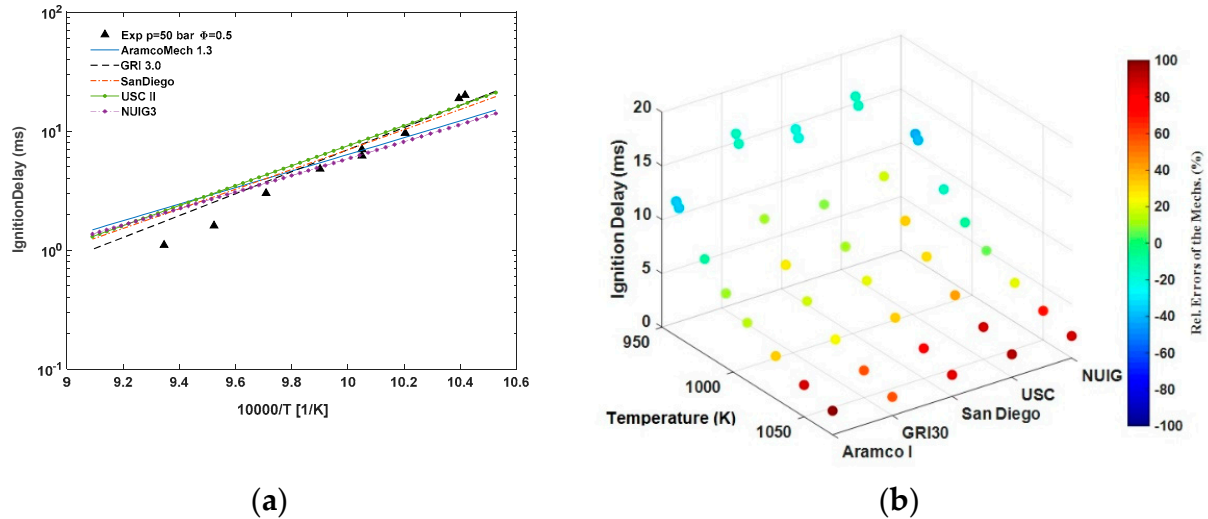

Figure 6. (**a**) Comparison of ignition delay time with the experimental data for $50\%CH_4/30\%H_2/20\%CO$ for different mechanisms [40]; (**b**) The relative error of simulation from experiments.
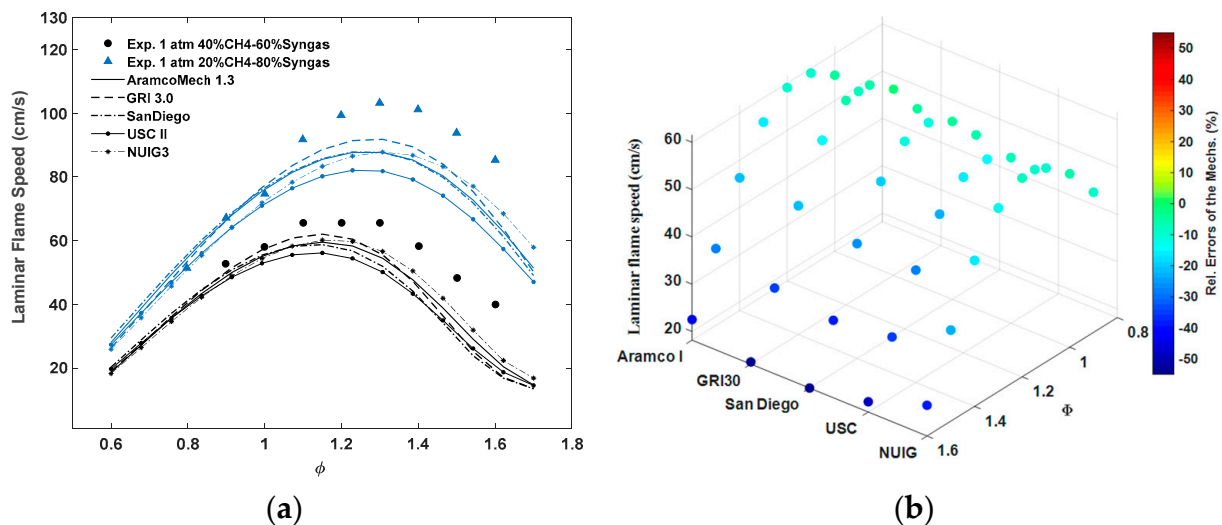

Figure 7. (**a**) Comparison of laminar flame speed with the experimental data of $CH_4/H_2/CO$ mixtures [43]; (**b**) The relative error of simulation from experiments.

3.3. Methane/Propane Mixtures

Simulations of the ignition delay time of methane/propane mixtures, particularly at pressures and concentrations of interest to IC engines, are therefore important for the design of efficient engines and optimization of chemical kinetics models. Figure 8 demonstrates the results of ignition delay times comparison of methane/propane mixtures at different pressures. It can be seen that in the case of high propane volume fraction and at high pressures and low temperatures, NUIG mechanism has good predictions. At low propane fractions and at high pressures and temperatures GRI-3.0 and USC II mechanisms provided better results.
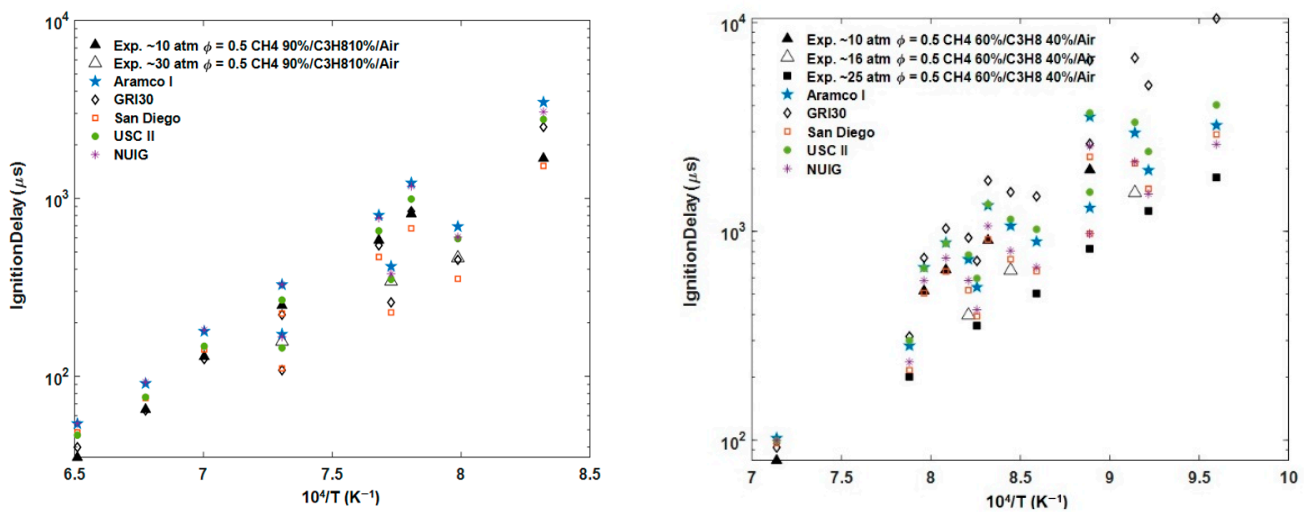
Figure 8. Comparison of ignition delay times of CH_4/C_3H_8 mixtures with experimental data at $\Phi = 0.5$ and different pressures: **Left**: $90\%CH_4/10\%C_3H_8$; **Right**: $60\%CH_4/40\%C_3H_8$ [41].

3.4. Effect of Pressure and Equivalence Ratio on Methane/Syngas Ignition Delay Times and Laminar Flame Speeds

Figure 9 shows the variation of ignition delay versus equivalence ration for the mechanisms in two different constant temperatures ($T = 1000$ K and 1600 K) and $p = 40$ bar pressure for methane/syngas ($50\%CH_4/30\%H_2/20\%CO$) mixture. It can be seen that ignition delay decreases at high temperatures due to acceleration in chain branching reactions. As expected, for lower temperatures, ignition delay time was decreasing by shifting from lean to rich mixtures; however, it has a different trend for high temperature conditions. The same ignition delay time dependency has been given by all five mechanisms at lower temperatures while changing the equivalence ratio, with NUIG provided a 1.5 factor underestimation relative to GRI-Mech 3.0. At higher temperatures, as the equivalence ratio increases towards stoichiometric condition, ignition delay time reduces, and then it starts increasing. In fact, the minimum ignition delay time can be achieved at stoichiometric condition in this case. Additionally, GRI-Mech 3.0 gives the lowest values of ignition delay time. Meanwhile USC and UCSD mechanisms show a greater dependence to equivalence ratio.
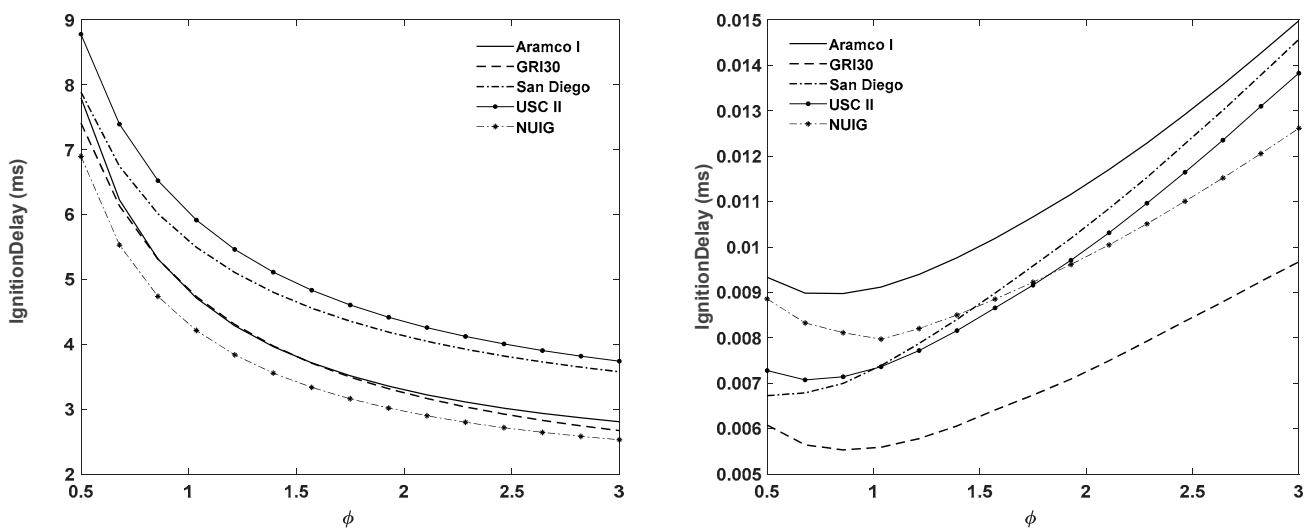

Figure 9. Ignition delay time calculated from all mechanisms at $p = 40$ bar and at different equivalence ratio values for methane/syngas mixture, **left**: $T = 1000$ K; **right**: $T = 1600$ K.

3.5. Ignition Delay Times and Laminar Flame Speeds of Methane/Syngas Mixtures with Reduced Mechanisms

As previously described, ignition delay times and laminar flame speeds of methane-based mixtures will be estimated at pressures of up to 10 atm, by the GRI 3.0 mechanism [45,46]. The in-cylinder pressure in SI engines ranges from 10 bar (low load) to 40 bar (high load), and it can ascend to 150 bar after combustion initiation. It was already reported that at elevated pressures, Aramco 1.3 mechanism gives good predictions of ignition chemistry of methane-based fuels [23]. However, in engine optimization problems, it is crucial to use reduced mechanisms with low number of species and reactions in order to decrease computational cost [47–49]; thus, two new mechanisms were selected for comparison with GRI 3.0 mechanism. In this part, GRI-3.0 mechanism, reduced Aramco 1.3 mechanism (i.e., 290Rxn mechanism consisting of 72 species and 290 reactions) [31] and Wang's mechanism (consisting of 56 species and 428 reactions) [33] were selected for comparison of ignition delay times and laminar flame speeds. Figure 10 shows that by increasing the pressure to higher than 50 bar, the 290Rxn mechanism has superior predictions of ignition delay times for methane/syngas mixtures.
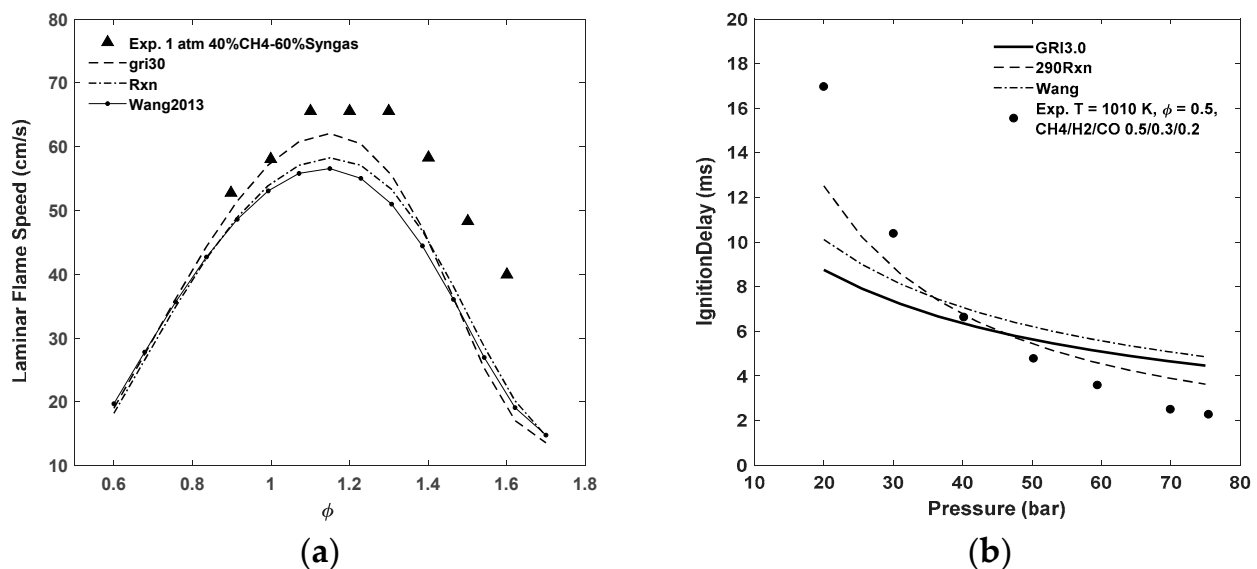

Figure 10. (**a**) Comparison of laminar flame speeds of $CH_4/H_2/CO$ blend at p = 1 atm with experimental data [43]; (**b**) Ignition delay times versus pressure for $CH_4/H_2/CO$ blend at different pressures using GRI 3.0, 290Rxn, and Wang mechanisms.

Overall, it can be seen that there is a good agreement with the experiments at high pressures and lean mixtures corresponding to SI engine-like conditions for methane/syngas mixtures. For laminar flame speed due to the lack of data, just low-pressure case (p = 1 atm) was studied and the simulation results were satisfactory at lean conditions. In general, 290Rxn mechanism can predict well the ignition delay times and laminar flame speeds at high pressures; therefore, it was selected as the chemical kinetics mechanism for simulations in the present study.

3.6. Effect of Hydrogen Addition on Methane's Ignition Delay Times and Laminar Flame Speeds

The effect of hydrogen addition on methane ignition delay times versus pressure and equivalence ratio differences, at two various temperatures, has been indicated in Figure 11. On account of high reactivity, high diffusion, and low auto-ignition temperature, the ignition delay time decreases as pressure and hydrogen volume fraction increase [50]. At lower hydrogen volume fractions, the effect of pressure on CH_4/H_2 fuel blend ignition is more noticeable. The impact of various hydrogen volume fractions on the ignition delay period of methane at T = 900–1300 K has been indicated in Figure 12. It is inter-

esting to note that by increasing hydrogen volume fraction up to 0.4, ignition delay time increases first at T = 900 K, and then it starts declining which is in consistent with the reported results in the literature [40]. At low temperatures (T < 1000 K), the dominant chain branching reactions in methane/hydrogen ignition chemistry are to blame. At low temperatures, the HO_2 radical plays a large role in ignition chemistry, and the chain termination reaction ($H + O_2(+M) \Leftrightarrow HO_2(+M)$)wins out over the chain branching reaction ($H + O_2 \Leftrightarrow OH + O$), which avoid ignition, slows reaction rate, and lengthens ignition delay [51].

Figure 13 depicts the influence of hydrogen addition on laminar flame speeds of methane at different pressures and equivalence ratios. As expected, by decreasing pressure and increasing hydrogen volume fraction, laminar flame speed enhances. This increment is significant at higher equivalence ratios and hydrogen volume fractions. It is interesting to note that effect of hydrogen fraction is much prominent at higher equivalence ratios, indeed laminar flame speed was not affected by hydrogen addition at ϕ = 0.5. Therefore, combination of H_2 volume fraction and equivalence ratio has considerable effect on methane's laminar flame speed.
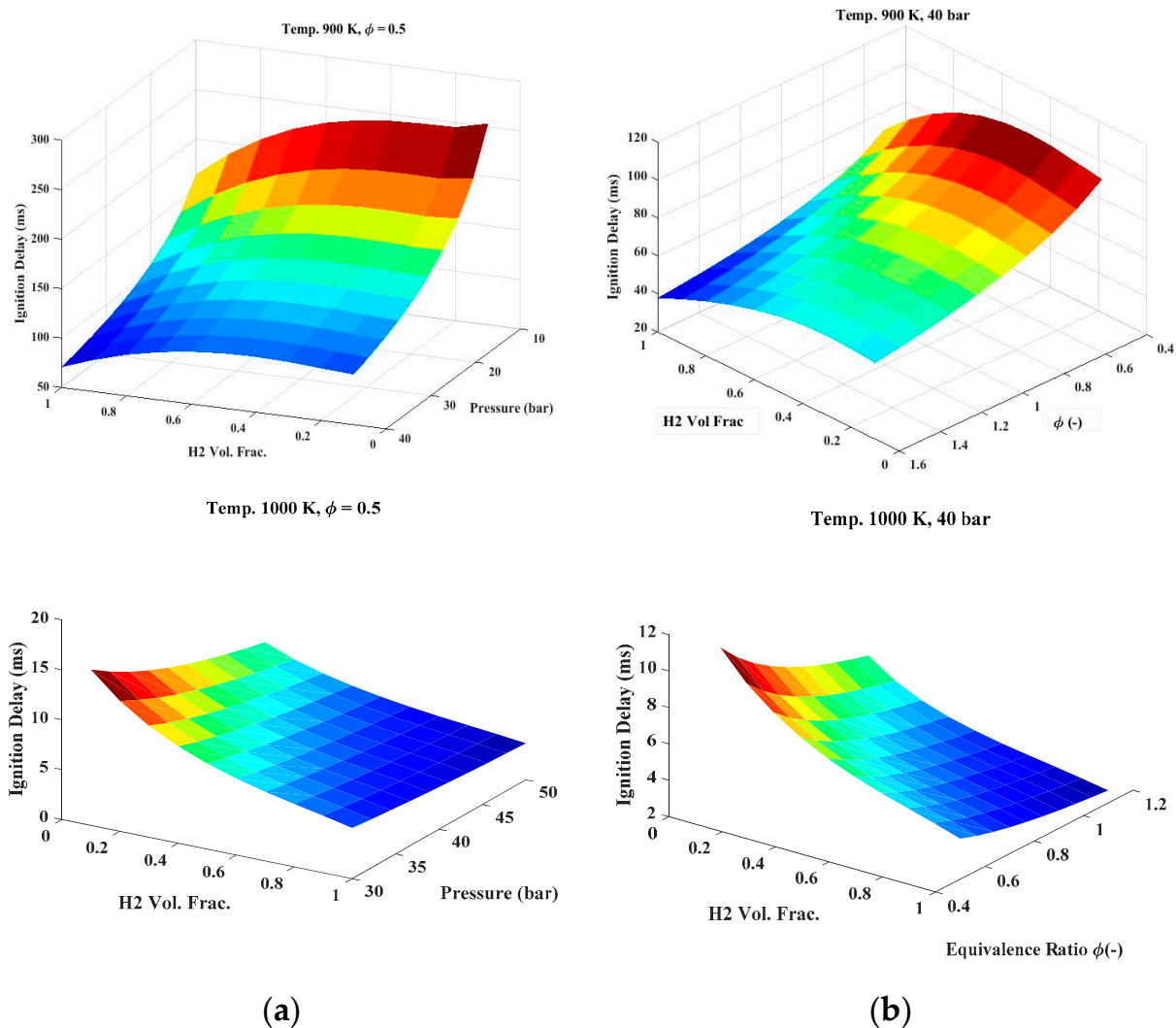

Figure 11. Effect of H_2 addition on methane's ignition delay times at: (**a**) different pressure at T = 900 and 1000 K, Φ = 0.5; (**b**) different equivalence ratios at T = 900 and 1000 K, p = 40 bar.
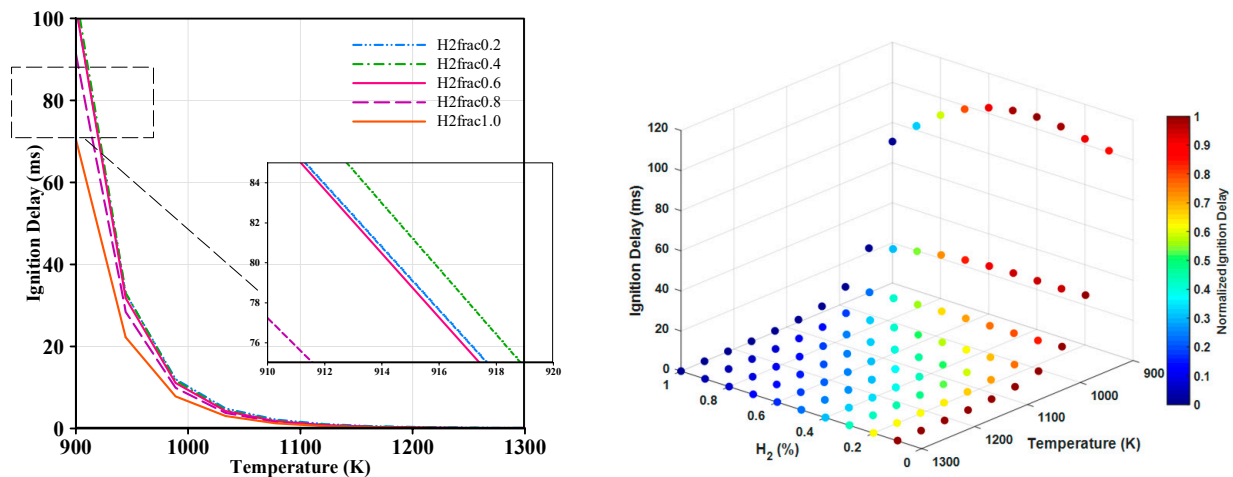
Figure 12. Effect of H_2 addition on methane's ignition delay times at different temperatures at *p* = 40 bar (right image shows the normalized ignition delay time error for each case).
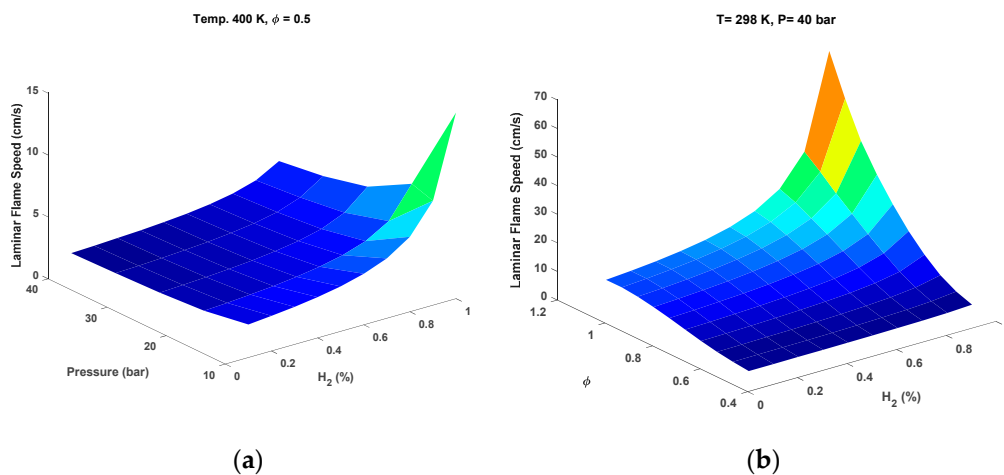

Figure 13. Effect of H_2 addition on methane's laminar flame speeds at: (**a**) different pressure at *T* = 400 K, *Φ* = 0.5; (**b**) different equivalence ratios at *T* = 298 K, *p* = 40 bar.

3.7. NOx and CO Emissions for Methane/Hydrogen and Methane/Syngas Cases

Figure 14 illustrates the NOx and CO emissions predicted by homogeneous reactor simulations performed at constant temperature and pressure for different temperatures and initial mixture equivalence ratios for methane/hydrogen and methane/syngas scenarios, for various temperatures and initial mixture equivalence ratios. The constant pressure conditions considered for these calculations are an approximation to a heterogeneous engine environment characterized by changing temperature, pressure, and continuous mixing. It is evident that the regions encountering high NOx and CO emissions are almost similar in both cases. NOx emissions start to increase to higher levels at *T* > 1800 K and lean blends, while high CO values are found at *T* > 1200 K and rich blends. It can be seen that for lean blends, the peak combustion temperature reaches the threshold temperature required for complete, rapid oxidation to occur. Thus, it can be concluded that for the studied cases at lean condition, NOx emission is a major issue and should be taken into account [52].
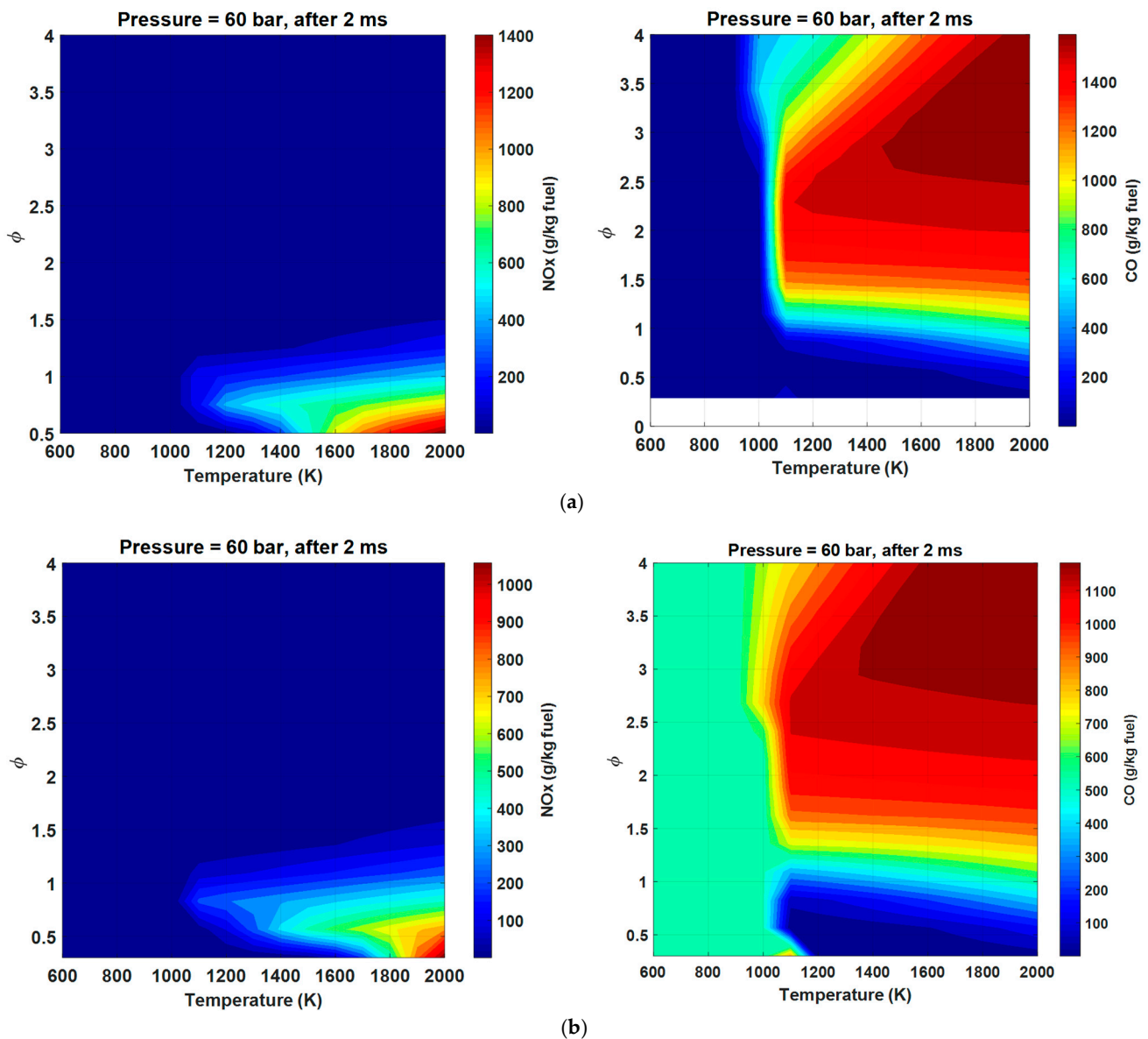
Figure 14. NOx and CO yield at 2.0 ms obtained from a homogeneous reactor simulation of: (**a**) 80%CH$_4$/20%H$_2$; (**b**) 40%CH$_4$/30%H$_2$/30%CO.

4. Conclusions

This study was carried out to find the suitable chemical kinetics mechanism that could be used to accurately predict the ignition characteristics of methane-based fuel blends under engine-relevant conditions. Overall, the agreement between the experiments and simulations results for all considered mechanisms was quite good. For pure methane case, a better estimation of predicted ignition delay time is obtained using GRI-Mech 3.0 at lean, lower temperatures, and high pressures. In addition, GRI 3.0 mechanism was found to yield the best performance for lean and stoichiometric condition for laminar flame speed prediction, while Aramco 1.3 and UCSD mechanisms provide more accurate results at rich conditions. Albeit its lower reaction numbers, the GRI 3.0 and 290Rxn mechanisms could predict accurate results of ignition chemistry for methane-based fuels under engine-relevant conditions, and due to their superiority in computational time, they can be used for 3D-CFD combustion simulation of natural gas-fueled SI engines. We believe that this work offers an important contribution to the natural gas combustion in SI engine industry.

Conflicts of Interest: The author declares no conflict of interest.

References

1. Korakianitis, T.; Namasivayam, A.; Crookes, R. Natural-gas fueled spark-ignition (SI) and compression-ignition (CI) engine performance and emissions. *Prog. Energy Combust. Sci.* **2011**, *37*, 89–112. [CrossRef]
2. Kakaee, A.-H.; Paykani, A.; Ghajar, M. The influence of fuel composition on the combustion and emission characteristics of natural gas fueled engines. *Renew. Sustain. Energy Rev.* **2014**, *38*, 64–78. [CrossRef]
3. Wang, X.; Khameneian, A.; Dice, P.; Chen, B.; Shahbakhti, M.; Naber, J.D.; Archer, C.; Qu, Q.; Glugla, C.; Huberts, G. Model-based combustion duration and ignition timing prediction for combustion phasing control of a spark-ignition engine using in-cylinder pressure sensors. In Proceedings of the International Design Engineering Technical Conferences and Computers and Information in Engineering Conference, Anaheim, CA, USA, 18–21 August 2019; American Society of Mechanical Engineers: New York, NY, USA, 2019; p. V009T12A033.
4. Kakaee, A.-H.; Paykani, A. Research and development of natural-gas fueled engines in Iran. *Renew. Sustain. Energy Rev.* **2013**, *26*, 805–821. [CrossRef]
5. Das, A.; Watson, H. Development of a natural gas spark ignition engine for optimum performance. *Proc. Inst. Mech. Eng. Part D J. Automob. Eng.* **1997**, *211*, 361–378. [CrossRef]
6. Rousseau, S.; Lemoult, B.; Tazerout, M. Combustion characterization of natural gas in a lean burn spark-ignition engine. *Proc. Inst. Mech. Eng. Part D J. Automob. Eng.* **1999**, *213*, 481–489. [CrossRef]
7. Wang, X.; Khameneian, A.; Dice, P.; Chen, B.; Shahbakhti, M.; Naber, J.D.; Archer, C.; Qu, Q.; Glugla, C.; Huberts, G. Control-oriented model-based burn duration and ignition timing prediction with recursive-least-square adaptation for closed-loop combustion phasing control of a spark ignition engine. In Proceedings of the ASME 2019 Dynamic Systems and Control Conference, Park City, UT, USA, 8–11 October 2019.
8. Khameneian, A.; Wang, X.; Dice, P.; Shahbakhti, M.; Naber, J.D.; Archer, C.; Moilanen, P.; Glugla, C.; Huberts, G. Model-Based Dynamic In-Cylinder Air Charge, Residual Gas and Temperature Estimation for a GDI Spark Ignition Engine Using Cylinder, Intake and Exhaust Pressures. In Proceedings of the Dynamic Systems and Control Conference, Online. 5–7 October 2020; American Society of Mechanical Engineers: New York, NY, USA, 2020; p. V002T26A002.
9. Ma, F.; Wang, Y. Study on the extension of lean operation limit through hydrogen enrichment in a natural gas spark-ignition engine. *Int. J. Hydrog. Energy* **2008**, *33*, 1416–1424. [CrossRef]
10. Kousheshi, N.; Yari, M.; Paykani, A.; Saberi Mehr, A.; de la Fuente, G.F. Effect of syngas composition on the combustion and emissions characteristics of a syngas/diesel RCCI engine. *Energies* **2020**, *13*, 212. [CrossRef]
11. Akansu, S.O.; Dulger, Z.; Kahraman, N.; Veziroğlu, T.N. Internal combustion engines fueled by natural gas—Hydrogen mixtures. *Int. J. Hydrog. Energy* **2004**, *29*, 1527–1539. [CrossRef]
12. Rahnama, P.; Paykani, A.; Reitz, R.D. A numerical study of the effects of using hydrogen, reformer gas and nitrogen on combustion, emissions and load limits of a heavy duty natural gas/diesel RCCI engine. *Appl. Energy* **2017**, *193*, 182–198. [CrossRef]
13. Rahnama, P.; Paykani, A.; Bordbar, V.; Reitz, R.D. A numerical study of the effects of reformer gas composition on the combustion and emission characteristics of a natural gas/diesel RCCI engine enriched with reformer gas. *Fuel* **2017**, *209*, 742–753. [CrossRef]
14. Karim, G.; Wierzba, I. Comparative studies of methane and propane as fuels for spark ignition and compression ignition engines. *SAE Trans.* **1983**, *92*, 676–688.
15. Merchant, S.S.; Goldsmith, C.F.; Vandeputte, A.G.; Burke, M.P.; Klippenstein, S.J.; Green, W.H. Understanding low-temperature first-stage ignition delay: Propane. *Combust. Flame* **2015**, *162*, 3658–3673. [CrossRef]
16. Schuh, S.; Ramalingam, A.K.; Minwegen, H.; Heufer, K.A.; Winter, F. Experimental Investigation and Benchmark Study of Oxidation of Methane–Propane–n-Heptane Mixtures at Pressures up to 100 bar. *Energies* **2019**, *12*, 3410. [CrossRef]
17. Hagos, F.Y.; Aziz, A.R.A.; Sulaiman, S.A. Methane enrichment of syngas (H_2/CO) in a spark-ignition direct-injection engine: Combustion, performance and emissions comparison with syngas and compressed natural gas. *Energy* **2015**, *90*, 2006–2015. [CrossRef]
18. Zabetakis, M.G. *Flammability Characteristics of Combustible Gases and Vapors*; Bureau of Mines: Washington, DC, USA, 1965.
19. Spadaccini, L.; Colket, M., III. Ignition delay characteristics of methane fuels. *Prog. Energy Combust. Sci.* **1994**, *20*, 431–460. [CrossRef]
20. Gersen, S.; Anikin, N.; Mokhov, A.; Levinsky, H. Ignition properties of methane/hydrogen mixtures in a rapid compression machine. *Int. J. Hydrog. Energy* **2008**, *33*, 1957–1964. [CrossRef]
21. Halter, F.; Chauveau, C.; Djebaïli-Chaumeix, N.; Gökalp, I. Characterization of the effects of pressure and hydrogen concentration on laminar burning velocities of methane–hydrogen–air mixtures. *Proc. Combust. Inst.* **2005**, *30*, 201–208. [CrossRef]

22. Hu, E.; Huang, Z.; He, J.; Jin, C.; Zheng, J. Experimental and numerical study on laminar burning characteristics of premixed methane–hydrogen–air flames. *Int. J. Hydrog. Energy* **2009**, *34*, 4876–4888. [CrossRef]
23. Hu, E.; Li, X.; Meng, X.; Chen, Y.; Cheng, Y.; Xie, Y.; Huang, Z. Laminar flame speeds and ignition delay times of methane–air mixtures at elevated temperatures and pressures. *Fuel* **2015**, *158*, 1–10. [CrossRef]
24. Lee, H.C.; Mohamad, A.A.; Jiang, L.-Y. Comprehensive comparison of chemical kinetics mechanisms for syngas/biogas mixtures. *Energy Fuels* **2015**, *29*, 6126–6145. [CrossRef]
25. Fischer, M.; Jiang, X. A chemical kinetic modelling study of the combustion of CH_4–CO–H_2–CO_2 fuel mixtures. *Combust. Flame* **2016**, *167*, 274–293. [CrossRef]
26. Goodwin, D.G.; Moffat, H.K.; Speth, R.L. Cantera: An Object-Oriented Software Toolkit for Chemical Kinetics, Thermodynamics, and Transport Processes, Version 2.2.1. 2016. Available online: https://www.cantera.org (accessed on 18 May 2019).
27. Healy, D.; Curran, H.; Simmie, J.; Kalitan, D.; Zinner, C.; Barrett, A.; Petersen, E.; Bourque, G. Methane/ethane/propane mixture oxidation at high pressures and at high, intermediate and low temperatures. *Combust. Flame* **2008**, *155*, 441–448. [CrossRef]
28. Healy, D.; Kalitan, D.; Aul, C.; Petersen, E.; Bourque, G.; Curran, H. Oxidation of C_1–C_5 alkane quinternary natural gas mixtures at high pressures. *Energy Fuels* **2010**, *24*, 1521–1528. [CrossRef]
29. Metcalfe, W.K.; Burke, S.M.; Ahmed, S.S.; Curran, H.J. A hierarchical and comparative kinetic modeling study of C_1–C_2 hydrocarbon and oxygenated fuels. *Int. J. Chem. Kinet.* **2013**, *45*, 638–675. [CrossRef]
30. Wang, H.; You, X.; Joshi, A.; Davis, S.; Laskin, A.; Egolfopoulos, F.; Law, C.K. USC Mech Version II. High-Temperature Combustion Reaction Model of H_2/CO/C1–C4 Compounds. May 2007. Available online: http://ignis.usc.edu/USC_Mech_II.htm (accessed on 18 May 2019).
31. Lee, H.; Mohamad, A.; Jiang, L. A detailed chemical kinetics for the combustion of H_2/CO/CH_4/CO_2 fuel mixtures. *Fuel* **2017**, *193*, 294–307. [CrossRef]
32. Williams, F. Chemical-Kinetic Mechanisms for Combustion Applications. Center for Energy Research, UCSD. 2003. Available online: http://maeweb.ucsd.edu/~{}combustion/cermech (accessed on 18 May 2019).
33. Wang, Q.-D. Skeletal mechanism generation for high-temperature combustion of H_2/CO/C_1–C_4 hydrocarbons. *Energy Fuels* **2013**, *27*, 4021–4030. [CrossRef]
34. Smith, G.P.; Golden, D.M.; Frenklach, M.; Moriarty, N.W.; Eiteneer, B.; Goldenberg, M.; Bowman, C.T.; Hanson, R.K.; Song, S.; Gardiner, W.C., Jr. GRI 3.0 Mechanism. Gas Research Institute. 1999. Available online: http://www.me.berkeley.edu/gri_mech (accessed on 18 May 2019).
35. Leschevich, V.; Martynenko, V.; Penyazkov, O.; Sevrouk, K.; Shabunya, S. Auto-ignitions of a methane/air mixture at high and intermediate temperatures. *Shock Waves* **2016**, *26*, 657–672. [CrossRef]
36. Hashemi, H.; Christensen, J.M.; Gersen, S.; Levinsky, H.; Klippenstein, S.J.; Glarborg, P. High-pressure oxidation of methane. *Combust. Flame* **2016**, *172*, 349–364. [CrossRef]
37. Petersen, E.; Davidson, D. Ignition delay times of ram accelerator mixtures. In Proceedings of the 32nd Joint Propulsion Conference and Exhibit, Lake Buena Vista, FL, USA, 1–3 July 1996; p. 2681.
38. El Merhubi, H.; Kéromnès, A.; Catalano, G.; Lefort, B.; Le Moyne, L. A high pressure experimental and numerical study of methane ignition. *Fuel* **2016**, *177*, 164–172. [CrossRef]
39. Petersen, E.L.; Hall, J.M.; Smith, S.D.; de Vries, J.; Amadio, A.R.; Crofton, M.W. Ignition of lean methane-based fuel blends at gas turbine pressures. *J. Eng. Gas Turbines Power* **2007**, *129*, 937–944. [CrossRef]
40. Gersen, S.; Darmeveil, H.; Levinsky, H. The effects of CO addition on the autoignition of H_2, CH_4 and CH_4/H_2 fuels at high pressure in an RCM. *Combust. Flame* **2012**, *159*, 3472–3475. [CrossRef]
41. Petersen, E.L.; Kalitan, D.M.; Simmons, S.; Bourque, G.; Curran, H.J.; Simmie, J.M. Methane/propane oxidation at high pressures: Experimental and detailed chemical kinetic modeling. *Proc. Combust. Inst.* **2007**, *31*, 447–454. [CrossRef]
42. Rozenchan, G.; Zhu, D.; Law, C.; Tse, S. Outward propagation, burning velocities, and chemical effects of methane flames up to 60 atm. *Proc. Combust. Inst.* **2002**, *29*, 1461–1470. [CrossRef]
43. Lapalme, D.; Seers, P. Influence of CO_2, CH_4, and initial temperature on H_2/CO laminar flame speed. *Int. J. Hydrog. Energy* **2014**, *39*, 3477–3486. [CrossRef]
44. De Vries, J.; Petersen, E. Autoignition of methane-based fuel blends under gas turbine conditions. *Proc. Combust. Inst.* **2007**, *31*, 3163–3171. [CrossRef]
45. Goswami, M.; Derks, S.C.; Coumans, K.; Slikker, W.J.; de Andrade Oliveira, M.H.; Bastiaans, R.J.; Luijten, C.C.; de Goey, L.P.H.; Konnov, A.A. The effect of elevated pressures on the laminar burning velocity of methane+ air mixtures. *Combust. Flame* **2013**, *160*, 1627–1635. [CrossRef]
46. Herzler, J.; Naumann, C. Shock-tube study of the ignition of methane/ethane/hydrogen mixtures with hydrogen contents from 0% to 100% at different pressures. *Proc. Combust. Inst.* **2009**, *32*, 213–220. [CrossRef]
47. Paykani, A.; Frouzakis, C.E.; Boulouchos, K. Numerical optimization of methane-based fuel blends under engine-relevant conditions using a multi-objective genetic algorithm. *Appl. Energy* **2019**, *242*, 1712–1724. [CrossRef]
48. Paykani, A.; Frouzakis, C.E.; Boulouchos, K. Optimization of composition of methane/syngas mixtures at en-gine-relevant conditions: A NSGA-II coupled TOPSIS approach. In Proceedings of the 3rd General Meeting and Workshop on SECs in Industry of SMARTCATs Action, Prague, Czech Republic, 25–27 October 2017; European Cooperation in Science and Technology (COST): Brussels, Belgium, 2017; p. 5.

49. Kakaee, A.-H.; Jafari, P.; Paykani, A. Numerical Study of Natural Gas/Diesel Reactivity Controlled Compression Ignition Combustion with Large Eddy Simulation and Reynolds-Averaged Navier–Stokes Model. *Fluids* **2018**, *3*, 24. [CrossRef]
50. Zhang, Y.; Huang, Z.; Wei, L.; Zhang, J.; Law, C.K. Experimental and modeling study on ignition delays of lean mixtures of methane, hydrogen, oxygen, and argon at elevated pressures. *Combust. Flame* **2012**, *159*, 918–931. [CrossRef]
51. Gersen, S.; van Essen, M.; van Dijk, G.; Levinsky, H. Physicochemical effects of varying fuel composition on knock characteristics of natural gas mixtures. *Combust. Flame* **2014**, *161*, 2729–2737. [CrossRef]
52. Wang, J.; Huang, Z.; Tang, C.; Miao, H.; Wang, X. Numerical study of the effect of hydrogen addition on methane–air mixtures combustion. *Int. J. Hydrog. Energy* **2009**, *34*, 1084–1096. [CrossRef]